





# Scarless engineering of the *Drosophila* genome near any site-specific integration site

Siqian Feng <sup>1,2,\*</sup> Shan Lu <sup>2,3</sup> Wesley B. Grueber <sup>2,4,5</sup> and Richard S. Mann <sup>1,2,6,\*</sup>

<sup>1</sup>Department of Biochemistry and Molecular Biophysics, Columbia University, New York, NY 10032, USA

<sup>2</sup>Mortimer B. Zuckerman Mind Brain Behavior Institute, Columbia University, New York, NY 10027, USA

<sup>3</sup>Department of Biological Sciences, Columbia University, New York, NY 10027, USA

<sup>4</sup>Department of Neuroscience, Columbia University, New York, NY 10027, USA

<sup>5</sup>Department of Physiology and Cellular Biophysics, Columbia University, New York, NY 10032, USA

<sup>6</sup>Department of Systems Biology, Columbia University, New York, NY 10032, USA

\*Corresponding author: sf2607@columbia.edu (S.F.); rsm10@columbia.edu (R.S.M.)

## Abstract

We describe a simple and efficient technique that allows scarless engineering of *Drosophila* genomic sequences near any landing site containing an inverted attP cassette, such as a *MiMIC* insertion. This two-step method combines phiC31 integrase-mediated site-specific integration and homing nuclease-mediated resolution of local duplications, efficiently converting the original landing site allele to modified alleles that only have the desired change(s). Dominant markers incorporated into this method allow correct individual flies to be efficiently identified at each step. In principle, single attP sites and FRT sites are also valid landing sites. Given the large and increasing number of landing site lines available in the fly community, this method provides an easy and fast way to efficiently edit the majority of the *Drosophila* genome in a scarless manner. This technique should also be applicable to other species.

**Keywords:** genome engineering; *MiMIC*; *CRIMIC*; genome editing; *Drosophila*; *Hox*; *Antp*; *Ubx*; *Gr28b*

## Introduction

Reverse genetics is a powerful tool to study the functions of genes and proteins. To answer many important biological questions, it is necessary to make precise genomic changes at the base pair resolution, preferably in a scarless manner, such that the final alleles only have the desired mutation(s). It is therefore important to have simple and efficient techniques for scarless genome engineering.

The fruit fly *Drosophila melanogaster* is well known for its superior genetic tool kit. There have been many efforts to precisely engineer the *Drosophila* genome. The first successful attempt used so-called ends-in targeting by homologous recombination to generate a local duplication, followed by homing nuclease-mediated resolution of the duplication (Rong *et al.* 2002). The final mutant alleles are scarless, but because of the low efficiency of ends-in targeting, large-scale screening of thousands of vials is necessary to identify the successful targeting events. A variant technique called SIRT (Site-specific Integrase-mediated Repeated Targeting) is suitable for generating multiple different mutant alleles of the same locus (Gao *et al.* 2008). It involves an initial labor-intensive ends-in targeting step to insert an attP site near the locus of interest, but all subsequent mutagenesis uses highly efficient phiC31 integrase-mediated site-specific integration and homing nuclease-mediated resolution of the duplication. The final alleles generated by SIRT still have an attR scar.

RMCE (recombinase-mediated cassette exchange; Bateman *et al.* 2006)-based techniques represent a different strategy (Delker *et al.* 2019). In these approaches, the wild type locus is first replaced by an inverted attP cassette, two attP sites in the opposite orientation flanking a dominant marker. This is usually achieved by homologous recombination induced by cutting with a custom endonuclease such as ZFN, TALENs, or CRISPR. Next, phiC31 integrase-mediated RMCE is used to replace the dominant marker with a mutant version of the genomic sequence. RMCE-based techniques are relatively straightforward to perform and highly efficient, but the final alleles have two attR scars flanking the modifications.

Most recently, the CRISPR revolution has made the precise engineering of the animal genomes significantly easier. In *Drosophila*, to facilitate the identification of correctly engineered individuals, a dominant marker is often inserted into the genome as the wild type sequence is converted into the mutant sequence during CRISPR-mediated homologous recombination (Gratz *et al.* 2014). The dominant marker can later be removed, but a short scar such as an FRT site or a loxP site, is often left in the genome, although there are ways to remove the dominant marker in a scarless manner (for example with *piggyBac*, <https://flycrispr.org/>). In principal, scarless mutant alleles can also be directly generated by CRISPR-mediated homologous recombination. However, since most custom mutant alleles do not have easily observable

Received: December 03, 2020. Accepted: January 13, 2021

© The Author(s) 2021. Published by Oxford University Press on behalf of Genetics Society of America. All rights reserved.

For permissions, please email: journals.permissions@oup.com

phenotypes, individuals bearing the desired mutations must be identified by laborious molecular screening, and when the desired mutation only affects a few base pairs, or even a single base pair, PCR primers may not be able to distinguish the wild type and mutant sequences. In addition, a common challenge with CRISPR-based experiments is that the efficiency of the selected gRNA(s) is difficult to predict, and the rate of unsuccessful CRISPR attempts is not trivial (Kanca et al. 2019). Common strategies to increase gRNA efficiency are to test them in cell culture before injecting flies, or to generate gRNA expressing transgenic flies (Port et al. 2015), both of which require additional time and effort.

Here, we report a new approach that combines phiC31 integrase-mediated RMCE and homing nuclease-mediated resolution of local duplications to scarlessly engineer the *Drosophila* genomic sequences near any landing site with an inverted attP cassette. In this method, first a properly marked mutant DNA fragment is integrated into the selected landing site via RMCE. This creates local duplications on both sides of the integration sites, which are then resolved in a single step by homing nuclease-induced homologous recombination between the duplications, resulting in scarless mutant alleles. Previously, there have been some attempts to combine these two procedures for genome engineering. For example, Zolotarev et al. (2019) resolved one side of an RMCE allele in a scarless manner, whereas the other side still had a scar. Vilain et al. (2014) resolved the two sides one at a time to make scarless alleles, but this method did not include any visible marker, and relied entirely on molecular methods to identify the desired mutation. To our knowledge, there have been no reports describing the simultaneous resolution of both sides after RMCE, which significantly shortens the time required to generate the final scarless allele. Once an RMCE line has been generated, our method takes <2 months to obtain a final scarless allele.

Because of the large number of fly lines with inverted attP cassettes, a significant portion of the *Drosophila* genome is accessible with this technique. There are about 17,500 MiMIC insertion lines (Venken et al. 2011; Nagarkar-Jaiswal et al. 2015; Lee et al. 2018), and 7441 have been mapped. The mapped MiMIC insertions allow approximately half of the euchromatic *Drosophila* genome to be efficiently engineered with this method (see 'Discussion'). The fact that single attP sites and FRT sites are also potential landing sites further expands the accessible portion of the fly genome. phiC31 integrase-mediated site-specific recombination, such as RMCE, has been proven to be robust and efficient, and does not have the risk associated with CRISPR gRNA selection. We show that this technique can be used to efficiently make precise protein coding mutations as well as large insertions and deletions. This technique requires no laborious screening and efficiently generates the desired scarless alleles in a short period of time.

## Materials and methods

### Materials

Restriction enzymes, CIP, Klenow fragment, T4 DNA polymerase and T4 DNA ligase were purchased from the New England Biolabs. Oligos were all purchased from Fisher Scientific. DH5alpha (competent cells made in house), and Stbl2 cells (Invitrogen 10268019) were the *Escherichia coli* strains used for cloning. TALEN plasmids were designed by and purchased from University of Utah Mutation Generation and Detection Core Facility. DNA Molecular Weight Marker II, DIG-labeled (Roche

11218590910) was used as marker for all Southern blot experiments.

### Commercial reagents

AmpliScribe SP6 Transcription Kit (Epicentre AS3106).  
ScriptCap m<sup>7</sup>G Capping System (Cellscript C-SCCE0625).  
DIG High Prime DNA Labeling and Detection Starter Kit II (Roche 11585614910).  
DIG Wash and Block Buffer Set (Roche 11585762001).  
Vectashield mounting medium with DAPI (Vector Laboratories H-1200).

### Plasmids

pBluescript II KS(+).  
pUAST (Brand and Perrimon 1993).  
pUASTattB (Bischof et al. 2007).  
p[sChFP] (Abreu-Blanco et al. 2012).  
pUChsneo-Act (DGRC 1210; Thummel et al. 1988).  
pH-Stinger (DGRC 1018; Barolo et al. 2000).  
The MiMIC vector pMiLR-attP1-2-yellow-SA-EGFP (DGRC 1321) (Venken et al. 2011).  
pXLBacII-pUbdDsRed-T3 (a gift from Al Handler; Handler and Harrell 2001).  
pJFRC19-13XLexAop2-IVS-myr::GFP (Addgene plasmid No. 26224).

### Flies

#### From Bloomington:

5905 (isogenic  $w^{1118}$ ),  
6936 ( $P\{v, hs-I-CreI\}; ry^{506}$ ),  
19139 ( $w^{1118}, P\{w[+mC]=XP\}Ubx^{d00281}/TM6B, Tb^1$ ),  
36313 ( $y^1, M\{RFP[3xP3.PB] GFP[E.3xP3]=vas-int.B\}ZH-2A w^*$ ;  
 $Sb^1/TM6B, Tb^1$ ),  
28877 ( $lig4$ ),  
24482 ( $y^1, M\{RFP[3xP3.PB] GFP[E.3xP3]=vas-int.Dm\}ZH-2A w^*$ ;  
 $M\{3xP3-RFP.attP\}ZH-51C$ ),  
33187 ( $Antp^{M102272}$ ),  
55598 ( $MI11240$ ).

#### From the fly community:

$w^-$ ;  $P\{v, hs-I-SceI\}, Sco/CyO$  (a gift from Yikang Rong).

### Antibodies

The following primary antibodies were used in this study: mouse anti-FLAG clone M2 (Sigma F1804) and chicken anti-GFP (abcam ab13970). The following secondary antibody were used: 488-Goat anti-mouse IgG (Molecular Probes A11029) and 488-Goat anti-chicken IgY (Invitrogen SA5-10070).

## Methods

### The design and optimization of the targeting vectors

Three variants of the targeting vector were designed, one for use with landing sites containing an inverted attP cassette (pTargeting-RMCE), which had from the left to the right the following elements: attB-FRT, I-CreI-mini-white-I-CreI, multiple cloning site (MCS), I-SceI-hsneo-3xP3-RFP-I-SceI, attB (Supplementary Figure S1A). The other two vectors were for use with landing sites with a single attP or FRT site [pTargeting-(+) and pTargeting-(-)], which did not have the right most attB element, and differ by the orientation of the left most attB-FRT element relative to other elements in the vectors. It is worth noting that for the FRT sequence, both orientations have been defined as "positive" by different researchers, so it is important to inspect the actual FRT sequence in the landing site. In addition, the 3xP3-

RFP marker in all targeting vectors has a single loxP site (irrelevant to genome editing), which was present in the PCR template from which the 3xP3-RFP marker was amplified.

The initial pTargeting-RMCE vector was used to generate a targeting plasmid to engineer the *Antp* locus using the *Antp*<sup>M102272</sup> MiMIC insertion as the landing site, and RMCE events were identified by the loss of the *yellow* marker, which marks the original MiMIC insertion. The *hs-neo* marker worked as expected, conferring G418 resistance to the RMCE flies. However, there was only very weak RFP expression in the eyes, and no *white* expression could be detected. The weak RFP expression was due to the upstream *hs-neo* element, which is expected to be transcribed through the 3xP3-RFP marker gene because it did not have a transcription termination signal. This problem was solved by adding an SV40-polyA element downstream of *hs-neo* and upstream of 3xP3-RFP. This SV40-polyA element was included in all subsequent targeting vectors.

The lack of *mini-white* expression is most likely due to it being silenced in the *Antp* locus. The main evidence supporting this explanation is that all *mini-white* insertions that are expressed within the *Antp* locus are flanked by insulator elements. A similar observation was also seen in the *Bithorax Complex*, where the *Hox* gene *Ubx* resides. Within the *Bithorax Complex*, all *mini-white* marked transposons also have insulated *mini-white*, while immediately outside of the *Bithorax complex*, both insulated and non-insulated *mini-white* genes are expressed. Consistently, the non-insulated *mini-white* marker is silenced when inserted into the majority of genomic loci (Handler and Harrell 1999; Horn et al. 2000). Insulated targeting vectors were thus generated, in which four *gypsy* insulators were added to each version of the vectors, two flanking *mini-white*, and two flanking *hsneo-3xP3-RFP*. There are repetitive sequences in the *gypsy* insulators, and two insulators near each other would make the plasmids unstable. Therefore, a ~2 kb spacer (from the *Drosophila yellow* gene) was inserted into the middle of the MCS in all insulated targeting vectors, to separate the right *mini-white* insulator from the left *hsneo-3xP3-RFP* insulator (Supplementary Figure S1A). Because of the presence of multiple insulators, *Stbl2 E. coli* cells, which increases the stability of plasmids with repetitive sequences, must be used to manipulate the insulated targeting vectors. All preps of targeting plasmids derived from insulated targeting vectors should be verified by restriction digestion verification before being used in injection, as plasmid rearrangement happens more frequently during the growing of large volume *E. coli* cultures.

The details of targeting vector cloning are in Supplementary File S1, and the sequences of all targeting vectors are in Supplementary File S3. These vectors have been deposited to the DGRC (*Drosophila* Genomics Resource Center), and the catalog numbers are: pTargeting-attB(-) (1530), pTargeting-attB(-)-insulated (1531), pTargeting-attB(+) (1532), pTargeting-attB(+)-insulated (1533), pTargeting-RMCE (1534), and pTargeting-RMCE-insulated (1535).

### The generation of the *Ubx* landing site line:

To generate a custom landing site in the *Ubx* locus between the ATG start codon and the W-motif codons, a pair of TALENs was designed. To avoid potential issues caused by natural polymorphisms, this *Ubx* region of the *lig4* strain (Bloomington #28877), which would be used in TALEN-mediated genome targeting, was PCR amplified and sequenced. The exact sequence in the *lig4* strain was sent to the University of Utah Mutation Generation and Detection Core Facility for identification of optimal TALEN target sites, and the most promising pair of TALENs was then

purchased. The TALEN target sequence is: TGCCCGTTAGACCCTCCGCCT-gcaccagattccc-AGTGGGCGCT ATTTGGA, in which the upper-case letters show the TALEN binding sites, and the lower-case letters indicate the spacer between the two binding sites.

The TALEN plasmids were linearized by restriction digestion and gel purified, and were used as templates for *in vitro* transcription using the AmpliScribe SP6 Transcription Kit (Epicentre AS3106). The mRNAs were then capped in a subsequent reaction using the ScriptCap m<sup>7</sup>G Capping System (Cellscript C-SCCE0625).

A vector, pCassette-ubiDsRed, was generated, which has an *ubiDsRed* marked inverted attP cassette flanked by two different MCSs for inserting homologous arms. *Ubx-N-L* and *Ubx-N-R* homologous arms were cloned into these two MCS sites to generate the pCassette-*Ubx-N* donor plasmid. A mixture of this donor plasmid (final concentration 500 ng/μl) and the two capped TALEN mRNAs (final concentration 400 ng/μl each) was injected into the blastoderm of *lig4* embryos (injection done by BestGene Inc.), and the desired homologous events were identified by strong ubiquitous DsRed expression in the F1 generation. Positive individuals were used to generate stocks and several independent stocks were verified by Southern blot and sequencing. One fully verified line was used as *Ubx* landing site line.

The sequences of the TALEN plasmids are in Supplementary File S3, and the detailed cloning steps for the landing site donor plasmid are in Supplementary File S1.

### Building suitable homing nuclease-expressing fly strains

Standard fly genetics was used to mobilize P element to obtain *hs-I-SceI(X)* and *hs-I-CreI(II)*. Because the *hs-I-SceI* transgene was marked with *vermillion (v)*, an attempt was made to generate the line *v*<sup>1</sup>; *P{v, hs-I-SceI}*, *Sco/CyO* for P element mobilization from the strain *w*; *P{v, hs-I-SceI}*, *Sco/CyO* (a gift from Yikang Rong). However, *v*<sup>1</sup>/(*FM7C*); *P{v, hs-I-SceI}*, *Sco/CyO* females were sterile, so instead, the line *v*<sup>1</sup>; *Pin, P{v, hs-I-SceI}/CyO* was generated, and was used as the starting line to jump *P{v, hs-I-SceI}* from chromosome II to X chromosome. The *P{v, hs-I-CreI}* P element was jumped to chromosome II from the X chromosome, using *v*<sup>1</sup>; *P{v, hs-I-CreI}*; *ry*<sup>506</sup> (Bloomington #6936) as the starting line.

X chromosome with the genotype *v*<sup>1</sup>; *P{v, hs-I-SceI}*, *P{v, hs-I-CreI}*, and chromosome II with the genotype *Pin, P{v, hs-I-SceI}*, *P{v, hs-I-CreI}* were then generated by recombination. *v+* recombinants were screened for the presence of both *hs-I-SceI* and *hs-I-CreI* transgenes by PCR using primer pairs *hs-I-SceI-5'* + *hs-I-SceI-3'*, and *hs-I-CreI-5'* + *hs-I-CreI-3'*, respectively. Finally, appropriate balancers were added by crossing.

All primer sequences are in Supplementary File S2.

### Cloning of the integrated fragments

For *Antp* and *Ubx* targeting, the integrated fragment was assembled from three subfragments, and the ~2 kb middle subfragment contained the loci to be mutated. The three subfragments were PCR amplified from genomic DNA and cloned into the pBluescript vector. Both the PCR products and the cloned fragments were fully sequenced to ensure no PCR-introduced mutations in the cloned fragments. The desired mutations were then introduced to the middle subfragment by standard procedures. Next, a three-fragment ligation was performed to assemble the complete integrated fragment in pBluescript. The assembled integrated fragment was then cloned into the targeting vector pTargeting-RMCE-insulated. For *Gr28b* deletion, a 2 kb left arm and a 2.3 kb right arm flanking the desired deletion were PCR

amplified from genomic DNA, digested with restriction enzymes, and ligated into pBluescript in a three-fragment ligation reaction. The 4.3 kb integrated fragment was then cloned into the targeting vector pTargeting-RMCE-insulated.

All detailed cloning steps are in Supplementary File S1.

### The identification and verification of RMCE alleles

All the landing site lines were verified before being used in injections. The *Ubx* landing site line was generated in this study, and was fully verified by Southern blot analysis and sequencing. For *Antp* and *Gr28b* targeting, MiMIC insertions were used as landing sites, and the presence of the desired MiMIC insertions was verified by PCR. Clean genetic sublines, which removed a linked lethal mutation, were derived from single *Antp*<sup>Mi02272</sup> chromosomes, and one was selected for all subsequent injections.

Initially, *vas-int(X)*; MiMIC stocks were generated and tested for injection, but the injected embryos suffered high fatality rates. Improved survival was obtained from injecting the F1 embryos of the crosses between the *vas-int(X)* females and landing site containing males. All injections were done by BestGene Inc. G0 adults from the injected embryos were individually crossed to suitable balancer stocks, and the F1 flies were screened for RMCE events. The RMCE alleles were identified by the presence of the *mini-white* marker, and the presence of 3xP3-RFP and the loss of the original landing site marker were then confirmed for all *white+* individuals. RMCE stocks were then established from individual flies with the correct marker patterns. The orientations of the RMCE lines were determined by PCR.

At first, RMCE alleles were verified by Southern blotting before they were used for resolution. Later, a more efficient procedure was used: several RMCE alleles with the correct marker patterns were subjected to resolution without Southern blot verification, and fewer individual cross IIs from each RMCE allele were set up. After getting all final mutant alleles, Southern blot analyses of the RMCE alleles were performed alongside with selected final mutant alleles. This arrangement also enables more independent mutant alleles to be obtained.

During injections, two classes of abnormal recombination events were observed. (1) Some transformants had both *mini-white* and 3xP3-RFP, but the original landing site marker (*yellow* or *ubiDsRed*) remained present. These events probably resulted from site-specific recombination between a single pair of attP and attB sites, whereas the other recombination events did not happen. Or maybe two different plasmids were integrated into the genome, each via one site-specific recombination event. (2) As mentioned in the 'Results' section, some transformants lost the landing site marker, but only *mini-white* was present, and no 3xP3-RFP was observed. This class was most likely because of spontaneous resolution of the right end during phiC31 integrase-mediated RMCE, in which double-stranded DNA (dsDNA) breaks were introduced within the attP and attB sites, and could have triggered homologous recombination. The RMCE transformants were usually selected by the presence of *mini-white*, and the presence of 3xP3-RFP and the absence of the landing site marker were confirmed later. Therefore, it is reasonable to expect that 3xP3-RFP+, *white-*, *yellow-(ubiDsRed-)* transformants also existed, but they were unidentified. Spontaneous resolution of both ends during RMCE might also happen at low frequency.

The primer sequences for verifying MiMIC and RMCE alleles are in Supplementary File S2.

### Resolving the RMCE alleles to generate the final mutant alleles, and the definition of productive cross IIs

The crosses to resolve RMCE alleles of different chromosomes are shown in Figures 3, 4A and Supplementary Figure S6. All crosses were performed at 25°C. The following describes details of the resolution steps for chromosome II or III targets. If the target is on the X chromosome, individual females must be used in cross IIs and cross IIIs, and some details should be adjusted accordingly.

For cross I, several vials of crosses were set up, and the flies were allowed to accommodate for a few days. The adults were then allowed to lay embryos for 72 h before being transferred to new vials, and the embryo/larvae in the old vials were heat shocked at 37°C. If I-SceI was the only homing nuclease expressed, 1-h heat shock was performed. A 20-min heat shock was performed if I-CreI was involved, either with or without I-SceI (Note: in the sequential resolution reported here, a 40-min heat shock was performed to induce I-CreI expression, but later results showed that a 20-min heat shock might give better efficiency). A second 72-h collection and heat shock might be performed if necessary. When the heat shocked individuals reach adult stage, males of the desired genotype were individually crossed to a balancer line in cross II. The progeny of cross IIs was screened once every 2–3 days for males that lost the desired marker(s). For simultaneous resolution, white-eyed males were first identified, and the 3xP3-RFP marker was then inspected under a fluorescent scope. Once male progeny that lost the desired marker(s) was identified from a cross II, this particular cross II was not screened further. To ensure all final alleles were independent, for each cross II, only one cross III was set up. If the selected individual male used in a cross III turned out to be sterile, no extra cross IIIs were set up for the corresponding cross II, even if that cross II might have produced more males that lost the desired marker(s).

For the purpose of easy scoring and comparison, a productive cross II was defined as an individual cross II that eventually generated a final stock. Occasionally, the selected single male from a cross II was sterile, and this particular Cross II would be scored as nonproductive. In some cases, the final stock from a Cross II might not be a correctly resolved allele (e.g., it might be a right marker deletion event), but such a cross II would be scored as productive according to the above definition.

### Southern blot analysis

Southern blots were performed using the DIG High Prime DNA Labeling and Detection Starter Kit II (Roche 11585614910) and the DIG Wash and Block Buffer Set (Roche 11585762001), according to manufacturer's instructions. DNA Molecular Weight Marker II, DIG-labeled (Roche 11218590910) was used as marker. In general, two probes were needed to verify the selected alleles. After hybridizing with the first probe, the blot was stripped and re-hybridized with the second probe according to manufacturer's instructions. For *Antp* and *Ubx* targeting, the left and right sub-fragments in the integrated fragment (see above) were used to generate DIG labeled 5' and 3' Southern blot probes. For *Gr28b* deletion, the left and right arms (see above) were used as templates to generate the probes.

### Sequencing of the mutant alleles

For all selected final mutant alleles, the genomic region corresponding to the integrated fragment in the targeting plasmid plus short (100–200 bp or so) flanking regions was completely



sequenced. For homozygous lethal alleles, embryos were collected overnight at 25°C from the balanced stock, and were further aged at 25°C for at least 30 h. Six unhatched embryos were randomly selected and single-embryo genomic DNA extraction was performed. A fragment covering the regions with desired mutation(s) was PCR amplified and sequenced to genotype the selected embryos. Homozygous mutant embryos were identified and their genomic DNA samples were used as PCR templates. For homozygous viable alleles, homozygotes were used to extract genomic DNA. The region to be sequenced was divided into 2–3 kb fragments with small overlaps. These fragments were PCR amplified with Phusion DNA polymerase, and gel purified before sequencing with sequence-specific primers. Gel purification was necessary to obtain high-quality sequencing results, especially if the genomic DNA was from single embryos.

In all the targeting cases reported in this study, there are natural polymorphisms between the landing site line and the line from which the donor fragment was PCR amplified. The pattern of polymorphisms in the resolved lines generally showed the expected pattern: the landing site-proximal regions often had the polymorphisms from the integrated fragments, while the landing site-distal regions usually had the polymorphisms from the original landing site line.

### Calculating the fraction of the fly genome accessible by our technique

The MiMIC mapping results were downloaded from the URL: <http://flypush.imgen.bcm.tmc.edu/pscreen/downloads.html>. The original file contains the base pair positions of 7441 MiMIC insertions. Eleven insertions with incomplete mapping information were dropped, and the rest 7430 MiMICs with complete mapping information were divided into 7311 euchromatic insertions and 119 heterochromatic insertions. For each group, a bed file containing 10 kb genomic intervals centered at every MiMIC insertion in that group was generated. Next, the “MergeBED” function in bedtools (performed on usegalaxy.eu) was used to generate two new bed files that contained merged nonredundant genomic intervals covering all sequences  $\leq 5$  kb from at least one MiMIC insertion. The lengths (in base pair) of each of these nonredundant genomic intervals were then calculated in Microsoft Excel. The total length of all 4093 nonredundant euchromatic intervals was calculated to be 56,673,025 bp, which is roughly half of the fly genome that is euchromatic (117 Mb; Hoskins et al. 2015). Since the mapped MiMIC lines represent only a subset of all available landing sites, and the estimate that 5 kb flanking a landing site can be engineered is a conservative one, the actual fraction of accessible euchromatic fly genome is expected to be significantly  $>50\%$ . The total length of all 66 nonredundant heterochromatic intervals was 887,350 bp.

### Embryo Staining

Embryo staining was performed using routine protocol. Briefly, the embryos were collected overnight and dechorionated with bleach. The dechorionated embryos were fixed with 1:1 mixture of heptane and 3.7% formaldehyde in 1×PBS for 20 min in room temperature with shaking. After fixation, the lower phase (formaldehyde in PBS) was removed and 1 volume of methanol was added. The samples were vigorously shaken for 1 min to remove the vitelline membrane. The fixed and devitellinized embryos were rehydrated by one 5-min wash with 1:1 mixture of PBST (1×PBS + 0.1% Triton X-100) and methanol, and two 5-min washes with PBST. Next, the rehydrated embryos were blocked with blocking solution (1% BSA in PBST) for 30 min with rotation.

The embryos were then incubated with primary antibody (1:1000 in blocking solution) with rotation at 4°C overnight. After three 30-min washes with PBST at room temperature, the embryos were incubated with secondary antibody (1:1000 in blocking solution) at room temperature in dark for 3 h with rotation. After another three 30-min washes with PBST in dark, the supernatant was removed, and several drops of the Vectashield mounting medium with DAPI (Vector Laboratories H-1200) were added to each sample. The samples were then left at 4°C overnight in dark to let the embryos settle. Finally, the embryos were mounted on slides and imaged with a Leica SP5 II confocal microscope. All images were processed using the Fiji software.

### Data availability

Tool flies generated in this study are available upon request. Targeting vectors generated in this study have been deposited to the *Drosophila* Genomics Resource Center (DGRC).

Supplementary material is available at <https://doi.org/10.25386/genetics.13611593>.

## Results

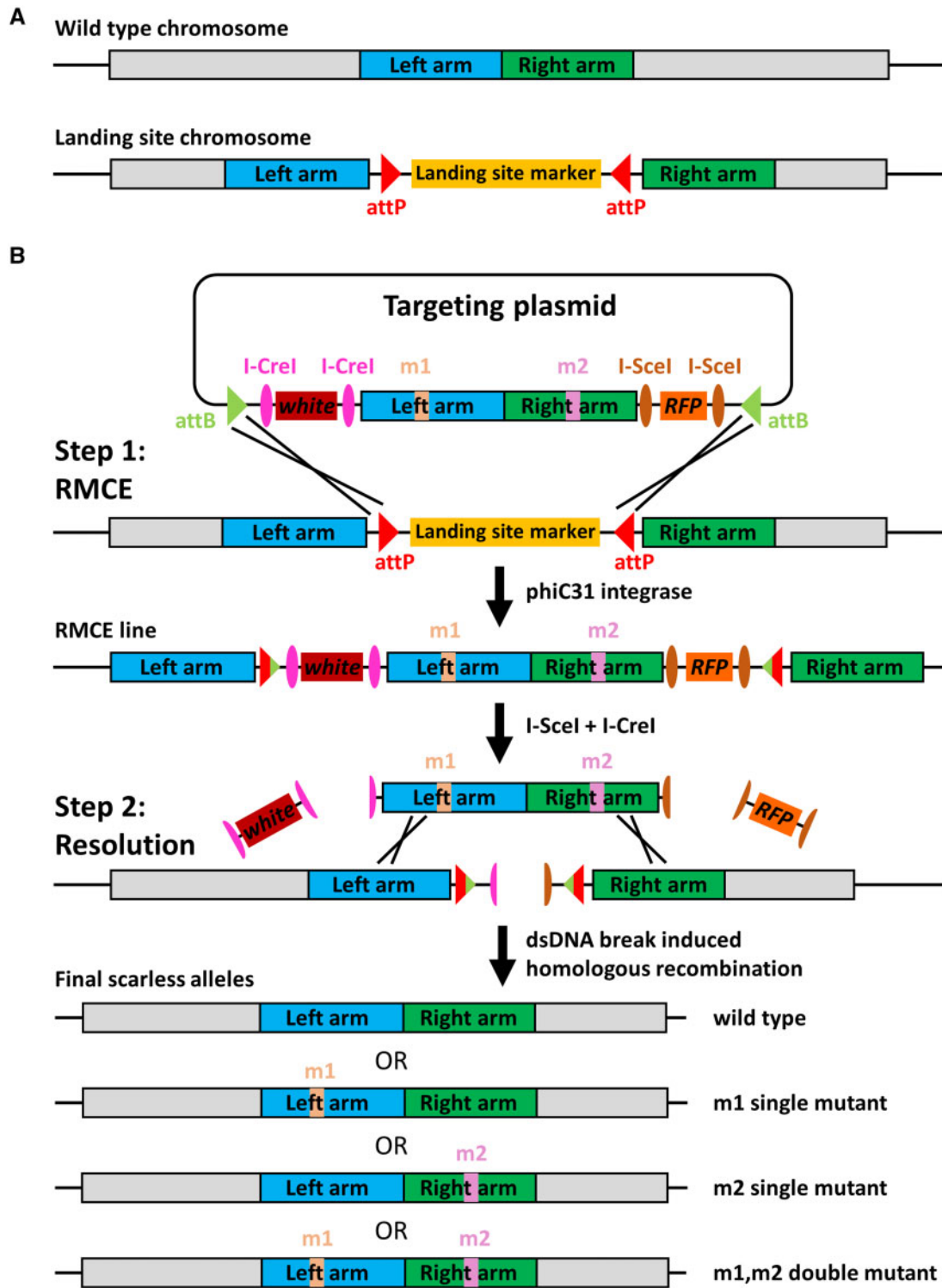
### Overall strategy

Figure 1 illustrates the overall two-step strategy of this method, exemplified using a landing site containing an inverted attP cassette, such as a MiMIC (Venken et al. 2011; Nagarkar-Jaiswal et al. 2015) or CRIMIC insertion (Lee et al. 2018). First, a fragment from the targeting plasmid is integrated into the selected landing site via RMCE. This fragment contains the desired mutation(s), and is flanked by dominant markers and homing nucleases sites. Second, the homing nucleases are expressed, and the resulting dsDNA breaks induce homologous recombination between the integrated mutant sequence and the original genomic sequences, thus resolving the locus to scarless mutant alleles. Alternatively, the two sides can be resolved sequentially (Supplementary Figure S1). In each step, desired individuals are identified by the presence or absence of dominant markers, which greatly simplifies the screening process. Importantly, the final alleles only have the desired mutation(s), with no additional modifications.

### Test of principle: engineering of the *Antp* locus by sequential resolution

The *Hox* gene *Antennapedia* (*Antp*) was selected for an initial test of this technique. There is a MiMIC insertion (*Antp*<sup>Mi02272</sup>) in the intron between the first coding exon and the small second coding exon, where the so-called W-motif is located (Figure 2A; Merabet and Mann 2016). The W-motif, also called the hexapeptide, is a protein-protein interaction motif present in nearly all Hox proteins that mediates the interaction between Hox proteins and their shared cofactor, the TALE family homeodomain protein [Extradenticle (Exd) in *Drosophila* and Pbx in vertebrates; Mann et al. 2009]. Although the functions of the W-motif have been extensively studied, most *in vivo* experiments rely on ectopic expression of mutant Hox proteins (Merabet and Mann 2016). Therefore, this motif represents an interesting target for *in vivo* genome engineering.

The *Antp*<sup>Mi02272</sup> MiMIC insertion is 1150 bp downstream of the ATG start codon, and 250 bp upstream of the W-motif codons (Figure 2A). Our goals were to insert a short 3×FLAG tag at the N terminus of the *Antp* protein and to mutate the W-motif from YPWM to AAAA (4 alanines; Figure 2C). To generate the targeting plasmid, a 7.8 kb genomic fragment flanking the MiMIC insertion



**Figure 1** Overall strategy of the genome editing method. (A) Schematics showing the wild type chromosome and the landing site chromosome. (B) Schematic that details the two-step genome editing strategy. In step 1, a properly marked DNA fragment with the desired mutation(s) is integrated near the locus of interest. In step 2, homologous recombination induced by homing nuclease generated dsDNA breaks resolves the local duplications, and generates the final scarless mutant alleles.

site, which had the N terminal 3xFLAG tag and the YPWM->AAAA mutation, was cloned into the optimized targeting vector, which contains the required markers and homing endonuclease sites (Figure 2B and Supplementary Figure S2). This targeting plasmid was injected into the F1 embryos of the cross between the MiMIC males and females from the *vas-int(X)* line, which

specifically expresses the phiC31 integrase in the germline (Bischof et al. 2007; see 'Materials and Methods' for details).

Successful RMCE events were identified by the presence of both *mini-white* and 3xP3-RFP markers, as well as the simultaneous loss of the yellow marker present in the original MiMIC insertion. PCR was performed to determine the orientation of the

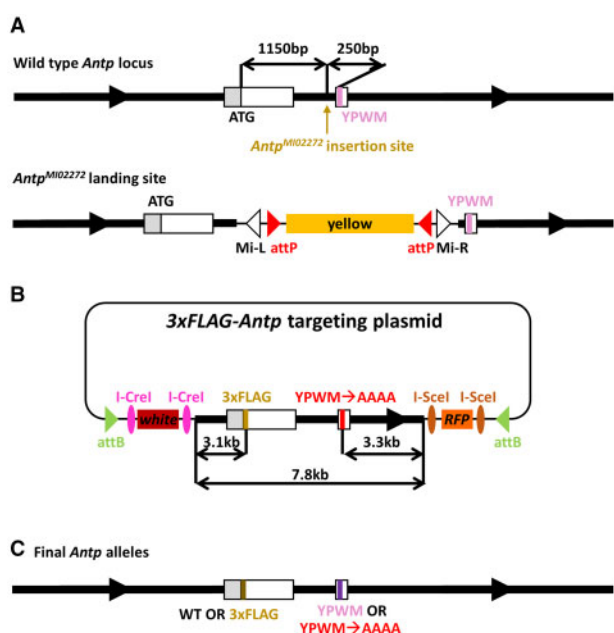


**Figure 2** Scarless engineering of the *Antp* locus. (A) The wild type *Antp* locus and the *Antp*<sup>MIO2272</sup> MiMIC landing site. The thick black lines denote introns and the arrows indicate the direction of transcription. The white boxes are coding exons, and the gray box shows part of the 5' UTR. The ATG start codon and the sequence encoding the W-motif, as well as their distances to the MiMIC insertion site, are indicated. (B) The *Antp* targeting plasmid. The total length of the integrated fragment, as well as the relative positions of the two desired mutations, are shown. (C) The final scarless alleles. The schematics in this figure are not drawn to scale.

RMCE lines. The entire targeting plasmid was about 20 kb in size, and a 17 kb fragment was integrated into the genome through RMCE. Despite the large size, multiple independent RMCE lines with the correct orientation were readily obtained. Due to the presence of insulators with repetitive sequences (see Supplementary Figure S2 and 'Materials and Methods'), Southern blot analysis was performed to ensure there were no unwanted rearrangements (Supplementary Figure S3). One fully verified RMCE line was selected for the next resolution step.

Prior to testing the simultaneous resolution of both sides, we first tested the sequential resolution of each side (Supplementary Figure S1). The right side was resolved first by expressing the homing endonuclease I-SceI (Figure 3A), which has an 18 bp recognition site that is not present in the *Drosophila* genome (Bellaiche et al. 1999). The *hs-I-SceI* flies were crossed to the RMCE flies (cross I) (Figure 3A), and their F1 embryos/larvae were heat shocked at 37°C for 1 h to induce I-SceI expression. 100 F1 adult males were then individually crossed to a balancer stock (cross II; Figure 3A). Every fertile cross II produced at least one male progeny that had lost the 3xP3-RFP marker, suggesting a high efficiency. To ensure all resolved lines were independent, only one male that lost 3xP3-RFP from each individual cross II was selected to generate a stock (cross III; Figure 3A).

In total, 94 independent RFP- lines were obtained, and 60 lines were randomly selected for Southern blot analysis. 41/60 lines showed the expected pattern of a successful resolution. The patterns of 18 of the other 19 lines were consistent with a marker deletion event induced by two dsDNA breaks flanking the 3xP3-RFP marker (Figure 3B and Supplementary Figure S4). Out of the 41 successfully resolved lines, 38 had the YPWM->AAAA mutation, and 3 were wild type, as determined by genotype-specific PCR.

The DNA sequence encoding the YPWM->AAAA mutation is 250 bp from the MiMIC insertion site and about 3300 bp from the end of the right homologous arm (Figure 2, A and B). Remarkably, the 3:38 observed wild type to mutant ratio is very close to expectations ( $250:3300 \approx 3:40$ ) if recombination is evenly distributed across the homology arm. Finally, we sequenced two wild type and two mutant alleles between the MiMIC insertion site and the end of the right homologous arm, and confirmed that no unwanted mutations were introduced.

Next, from fully verified right-side resolved lines, one wild type line and one mutant line were selected for left side resolution by I-CreI. The overall resolution strategy and crosses were essentially the same as for the right-side resolution (Figure 3C). I-CreI has endogenous target sites in the 28S rRNA gene in the heterochromatic regions on X and Y chromosomes (Rong et al. 2002), thus prolonged expression causes high rates of lethality and sterility. To reduce the toxicity of I-CreI, the heat shock was performed for 40 min at 37°C. Under such conditions, a mild reduction in fertility was observed in cross IIs, but each fertile cross II still produced at least one w- male. A slight reduction in fertility was also seen in cross IIIs (Figure 3D).

Ten fully resolved wild type lines and 20 fully resolved mutant lines were selected for further characterization. PCR was used to determine if the 3xFLAG tag was present, and to eliminate any marker deletion lines from further characterization. In total, 60% of the resolved lines had the 3xFLAG tag (Figure 3D), which was close to the expected ratio (~70%) based on the relative position of the ATG start codon in the integrated fragment (Figure 2, A and B). Five independent 3xFLAG-*Antp* alleles, four independent *Antp*(YPWM->AAAA) alleles, and 7 independent 3xFLAG-*Antp*(YPWM->AAAA) alleles were selected for Southern blot verification, and all gave the expected patterns (Supplementary Figure S5).

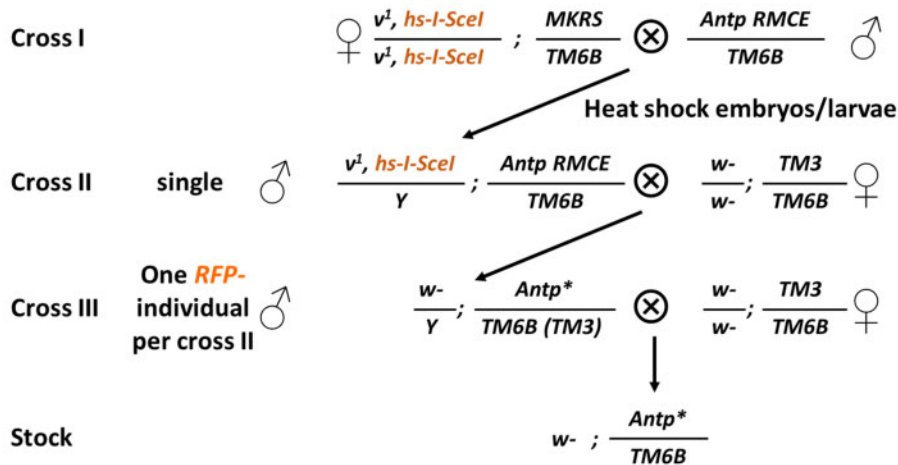
One noteworthy finding was that marker deletion events were not observed during left side resolution, either by PCR or by Southern blot, in contrast to right side resolution. Detailed inspection of the targeting vector revealed that the two I-SceI sites flanking the right side 3xP3-RFP marker were in the same orientation, such that the single stranded overhangs generated by I-SceI were compatible, thus facilitating a marker deletion event. In contrast, the two I-CreI sites flanking the left side *mini-white* marker were in the opposite orientation, thus the single stranded overhangs generated by I-CreI were not compatible, disfavoring simple marker deletion events. In this case and the following ones, we generally used long homologous arms (~2–3 kb) following older standard practice (Rong et al. 2002), but much shorter arms (0.5–1 kb) should also induce efficient homologous recombination (Beumer et al. 2013).

### Simultaneous resolution of both sides

Next, we tested the simultaneous resolution of both sides, which would significantly simplify and shorten the entire process (Figure 1B). The overall procedure was similar to left- or right-side resolution, except that both I-SceI and I-CreI were expressed together. The simultaneous resolution crosses for chromosome III targets are shown in Figure 4A, and those for chromosome II and X targets are shown in Supplementary Figure S6. We tested heat shock at 37°C for 10, 20, 30, and 40 min, and found that a 20-min heat shock gave the highest rate of productive cross II (data not shown), defined as the fraction of cross IIs that lead to a final stock (see Materials and Methods for more details).

To gain a better measure of the efficiency and robustness of this method, 8 different verified RMCE lines were subjected to simultaneous resolution (Figure 4B). After a 20-min heat shock,

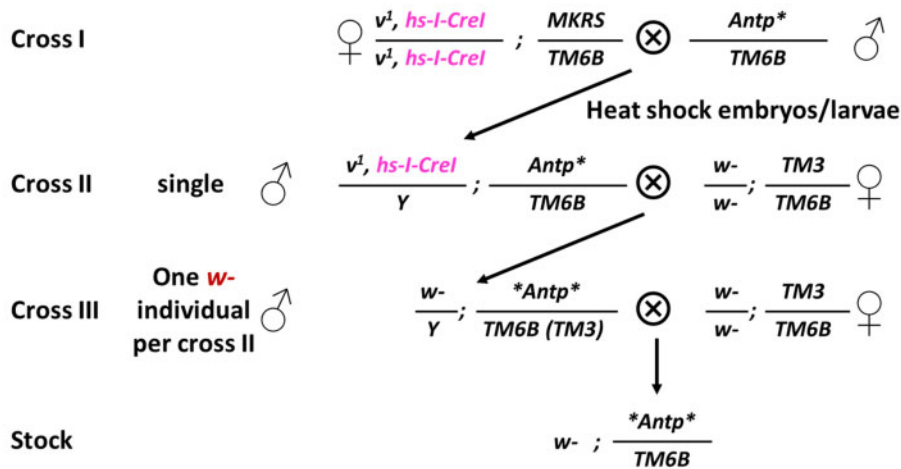
### A Crosses for *Antp* right-side resolution



### B

Cross II total	Cross II fertile (Cross III total)	Cross III fertile (Final alleles)	Southern tested alleles	Correct resolution	Marker deletion
100	99	94	60	41	18

### C Crosses for *Antp* left-side resolution



### D

Right side genotype	Cross II total	Cross II fertile (Cross III total)	Cross III fertile (Final alleles)	Genotyped by PCR	With 3xFLAG	No 3xFLAG
Wild type	25	23	13	10	6	4
YPWM→AAAA	75	54	45	20	12	8
Total	100	77	58	30	18	12

**Figure 3** Sequential resolution of the 3xFLAG-*Antp* RMCE allele. (A) The crosses for I-SceI-mediated right-side resolution of the 3xFLAG-*Antp* RMCE allele. (B) The results of I-SceI-mediated right-side resolution. Of the 94 independent final alleles, 60 were randomly selected for Southern blot analysis. (C) The crosses for I-CreI-mediated left-side resolution. (D) The results of I-CreI-mediated left-side resolution. 30 out of 58 final alleles were genotyped by PCR.

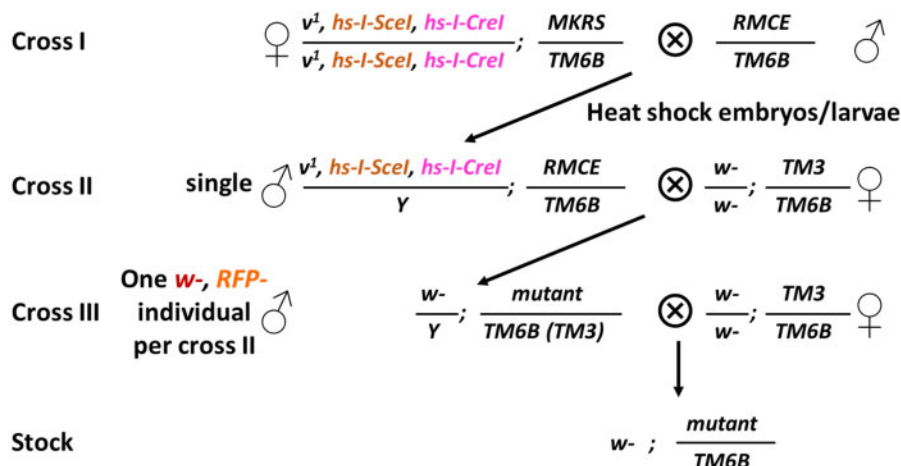
essentially normal viability and fertility were observed. On the other hand, not all individual cross IIs generated male progeny that lost both the *mini-white* and the 3xP3-RFP markers (Figure 4B); as expected, we frequently observed cross II progeny that lost either *mini-white* or 3xP3-RFP, but not both. Nevertheless,

except for one RMCE line (line F), the rate of productive cross II ranged from 50% to 70%, confirming the high efficiency of simultaneous resolution (Figure 4B).

We selected the final alleles resolved from three different RMCE lines for further characterization. PCR was first used to



### A Crosses for simultaneous resolution (chromosome III)



### B

Starting RMCE line	A	B	C	D	E	F	G	H (opposite)
Cross II total	50	50	50	50	50	50	50	50
Cross II fertile	45	47	50	50	47	46	45	49
Cross III total	26	30	35	35	39	19	29	40
Cross III fertile (Final alleles)	25	28	33	35	34	18	28	38
Productive cross II	50%	56%	66%	70%	68%	36%	56%	76%

### C

Starting RMCE line	Homozygous viable alleles		Homozygous lethal alleles				
	WT	3xFLAG-Antp	Antp(YPWM →AAAA)	3xFLAG-Antp(YPWM →AAAA)	Right marker deletion	Apparent 3xFLAG-Antp	Not genotyped
C	5	4	1	2	5	0	16
D	2	4	2	4	2	0	21
G	2	1	2	4	1	1	17
H(opposite)	6	3	N/D				29

### D

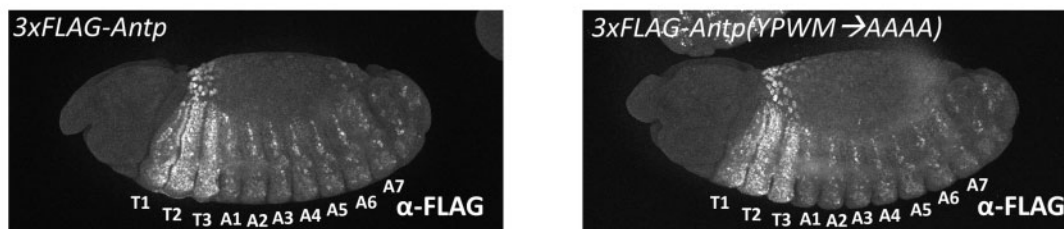


**Figure 4** Simultaneous resolution of 3xFLAG-Antp RMCE alleles. (A) Crosses for simultaneous resolution of RMCE alleles on chromosome III. (B) Results of the simultaneous resolution of 8 independent 3xFLAG-Antp RMCE alleles. RMCE allele H has the opposite integration orientation. (C). PCR genotyping results of selected final alleles from four starting RMCE alleles. For each genotype, multiple independent alleles were obtained. For RMCE allele H, which has the opposite orientation, only homozygous viable final alleles were genotyped. "N/D" stands for "not determined". (D) anti-FLAG staining of 3xFLAG-Antp and 3xFLAG-Antp(YPWM→AAAA) embryos. The embryos may be homozygous, or heterozygous with TM6B. Segments T1 to A7 are shown.

genotype the selected alleles. Because Antp's W-motif is expected to be necessary for viability, only the presence of the 3xFLAG tag was examined for all homozygous viable final alleles. For

selected homozygous lethal alleles, the presence of the 3xFLAG tag, the YPWM→AAAA mutation, as well as the potential right-side marker deletion were tested (Figure 4C). We detected some

right-side marker deletion events, as expected. One homozygous lethal allele had the apparent genotype of 3xFLAG-*Antp*/+. Presumably, an unwanted mutation occurred during resolution, which caused the observed homozygous lethality. Southern blot was performed on 15 genotyped alleles, and 14 gave the expected patterns (Supplementary Figure S7), confirming the high accuracy of this technique. Finally, all 14 Southern blot-verified lines were confirmed by sequencing, and contained no unwanted mutations. Antibody staining against the 3xFLAG tag also confirmed that the tagged *Antp* protein had the same embryonic expression pattern as the wild type *Antp* protein (Figure 4D; Carroll et al. 1986).

### RMCE lines with opposite integration orientation can be resolved efficiently

The observation that simultaneous resolution works well raised the possibility that successful resolutions can be obtained even if the original RMCE line was in the opposite orientation, where the duplicated arms are not adjacent to their endogenous homologous sequences. We considered this possibility because when both I-SceI and I-CreI are expressed, the entire integrated fragment is liberated from the chromosome and, in principle, could pair with homologous sequences regardless of the initial orientation. We tested this with an RMCE line in the opposite orientation (Figure 4B). Indeed, this line showed a resolution efficiency that was among the highest of all eight tested RMCE lines.

To confirm the accuracy of the final alleles, we further characterized all nine homozygous viable alleles generated from this particular RMCE line. Of these nine alleles, three had the 3xFLAG-*Antp* genotype, while the other 6 were untagged (Figure 4C). We selected 2 of the 3 3xFLAG-*Antp* alleles for further verification by Southern blotting, and both gave the expected patterns (Supplementary Figure S7). The sequences of these 2 alleles confirmed that there were no additional mutations.

### Precise editing of *Ubx*, another *Hox* gene

To test the generality of this method, we engineered another *Hox* gene, *Ultrabithorax* (*Ubx*). We chose to mutate the canonical W-motif, the YPWM motif, and insert an N terminal 3xFLAG tag (Figure 5, A and C). As no landing site insertions were available, we first inserted an inverted attP cassette marked with *ubi-DsRed* (Handler and Harrell 2001) into the *Ubx* locus, using a pair of custom TALENs that target the first coding exon of *Ubx* (Figure 5A; see *Materials and Methods* for details).

One fully verified *Ubx* landing site allele was selected as the starting strain for engineering the *Ubx* locus. A *Ubx* targeting plasmid was generated, which contained a 7.8 kb fragment with a 3xFLAG tag at the N terminal end of the *Ubx* ORF and the YPWM->AAAA mutation (Figure 5B). This targeting plasmid was injected into the F1 progeny of the *vas-int(X)* females and the *Ubx* landing site males, and multiple independent RMCE lines were obtained and further verified by Southern blot. One fully verified RMCE line was subjected to simultaneous resolution, following the same procedure as for the *Antp* locus. From 100 individual cross IIs, we were able to achieve a success rate of ~50% (Figure 5D).

Among the 49 alleles obtained, 22 were homozygous lethal, and 27 were homozygous viable (Figure 5E). 13 of the homozygous lethal alleles had the right marker deleted, as shown by PCR. All 4 expected genotypes, wild type, 3xFLAG-*Ubx*, *Ubx*(YPWM->AAAA) and 3xFLAG-*Ubx*(YPWM->AAAA), were identified from the 27 homozygous viable alleles (Figure 5E), indicating the YPWM motif of *Ubx* is not necessary for viability. Although this W-motif is deeply conserved, this result was not

unexpected because *Ubx* has multiple additional Exd-interaction motifs (Merabet et al. 2007; Lelli et al. 2011; Merabet and Mann 2016), which may be able to partially compensate for the functions of the canonical YPWM motif. Some homozygous lethal alleles did not show a PCR product with primers designed to detect right-side marker deletion events (Figure 5E). These alleles might have undergone imprecise homologous recombination, or the marker deletion might have been accompanied by additional deletions near the dsDNA breaks, such that the primer binding sites were destroyed.

Southern blotting was performed to verify 16 different alleles; of these, 3 showed abnormal patterns (Supplementary Figure S8) and they were discarded. Two Southern blot verified alleles of each genotype of interest were fully sequenced, and all six were correct. Anti-FLAG staining also confirmed the wild type expression pattern of the tagged *Ubx* proteins (Figure 5F; Dura and Ingham 1988). The precise engineering of the *Ubx* locus demonstrated again the efficiency and precision of this technique. Southern blot analysis was performed in all cases reported in this study, and abnormal patterns were occasionally discovered, suggesting that verifying genome engineering alleles by PCR only, which is a common practice, may not always be sufficient.

### Generating insertions

The above results show that this technique can be used to efficiently mutate small stretches of genomic DNA sequence, or to insert a small fragment into a desired genomic locus. To further test the ability of this technique to generate large custom insertions, we chose to tag the endogenous *Antp* protein with GFP (Figure 6B). A slightly different *Antp* targeting plasmid, in which the 3x-FLAG tag was replaced with a 750 bp GFP tag (with a flexible linker between the GFP and *Antp* ORFs), was generated (Figure 6A), and multiple independent RMCE lines were obtained. One Southern blot-verified RMCE line was then used as the starting line for simultaneous resolution. Because it was unclear if and how the large-sized insertion would affect the resolution success rate, we set up 100 individual cross IIs. Despite the presence of a large insertion, the resolution results had a high rate of success: 70% of cross IIs were productive (Figure 6C).

In total, 6 of the 70 final alleles were homozygous viable, from which 2 independent GFP-*Antp* alleles were obtained, as determined by PCR, while the other 4 alleles were wild type. Many *Antp*(YPWM->AAAA) and GFP-*Antp*(YPWM->AAAA) alleles were identified by PCR among the homozygous lethal alleles (Figure 6D). Several independent alleles of each genotype were selected for Southern blot verification (Supplementary Figure S9) and all gave the correct patterns. Sequencing results verified that all selected alleles were correct, and anti-GFP staining confirmed the correct expression pattern of the GFP-*Antp* fusion proteins (Figure 6E; Carroll et al. 1986).

### Generating deletions

Finally, to test the ability of this technique to create custom deletions, the 7.5 kb *Gr28b* gene was chosen to be deleted (Figure 7, A and C). *Gr28b* is a complex gustatory receptor locus that encodes five different isoforms, and has been shown to have multiple functions such as thermo-preference and toxin avoidance (Ni et al. 2013; Sang et al. 2019). A MiMIC insertion (MI11240) about 300 bp away from the right end of the *Gr28b* gene was used as the landing site for the targeted deletion (Figure 7A). A targeting plasmid was generated, which contained a 2 kb fragment to the left of the desired deletion, fused to a 2.3 kb fragment to the right of the desired deletion (Figure 7B). This plasmid was used to inject F1

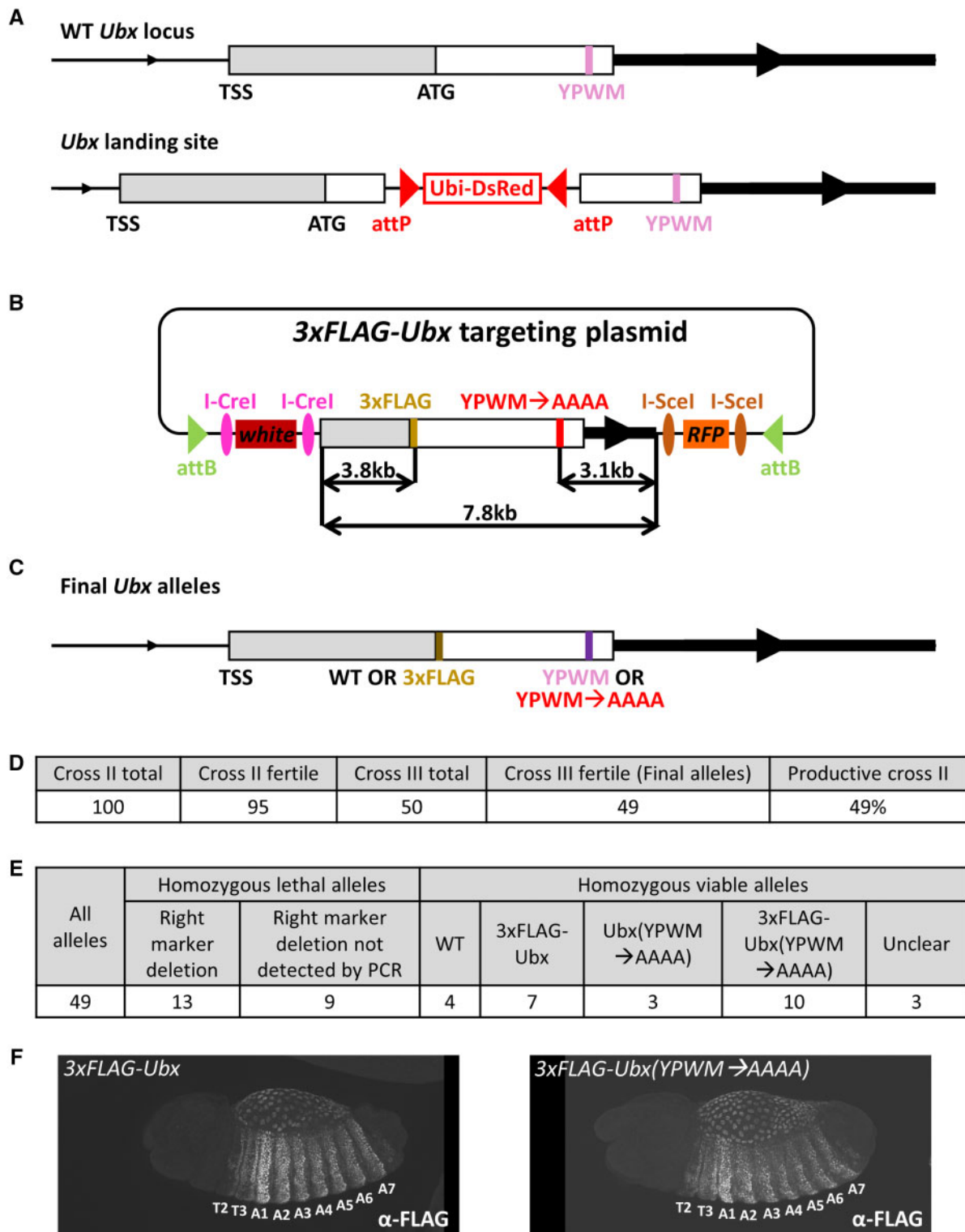


**Figure 5** Scarless engineering of the *Ubx* locus. (A) Schematics of the wild type *Ubx* locus and the *Ubx* landing site allele. (B) The targeting plasmid used in the scarless engineering of the *Ubx* locus. The desired mutations are shown, as well as their relative positions within the integrated fragment. (C) The desired final scarless alleles. The schematics in (A–C) are not drawn to scale. (D) Results of *Ubx* RMCE allele simultaneous resolution. (E) Genotyping results of all final *Ubx* alleles. “Unclear” refers to ambiguous genotyping results for 3 homozygous viable alleles. (F) Anti-FLAG staining of 3xFLAG-*Ubx* and 3xFLAG-*Ubx*(YPWM→AAAA) embryos. The embryos may be homozygous, or heterozygous with TM6B. Segments T2 to A7 are shown.

embryos of the cross between the *vas-int(X)* female and the MI11240 male, and multiple independent RMCE events were obtained. Unexpectedly, while some RMCE events landed on chromosome II, where the *Gr28b* gene is located, others did not

map to this chromosome. The presence of the MI11240 insertion in the original MiMIC stock was verified by PCR before it was used for injection, thus we hypothesized that the original MiMIC stock might have a secondary MiMIC insertion on a different

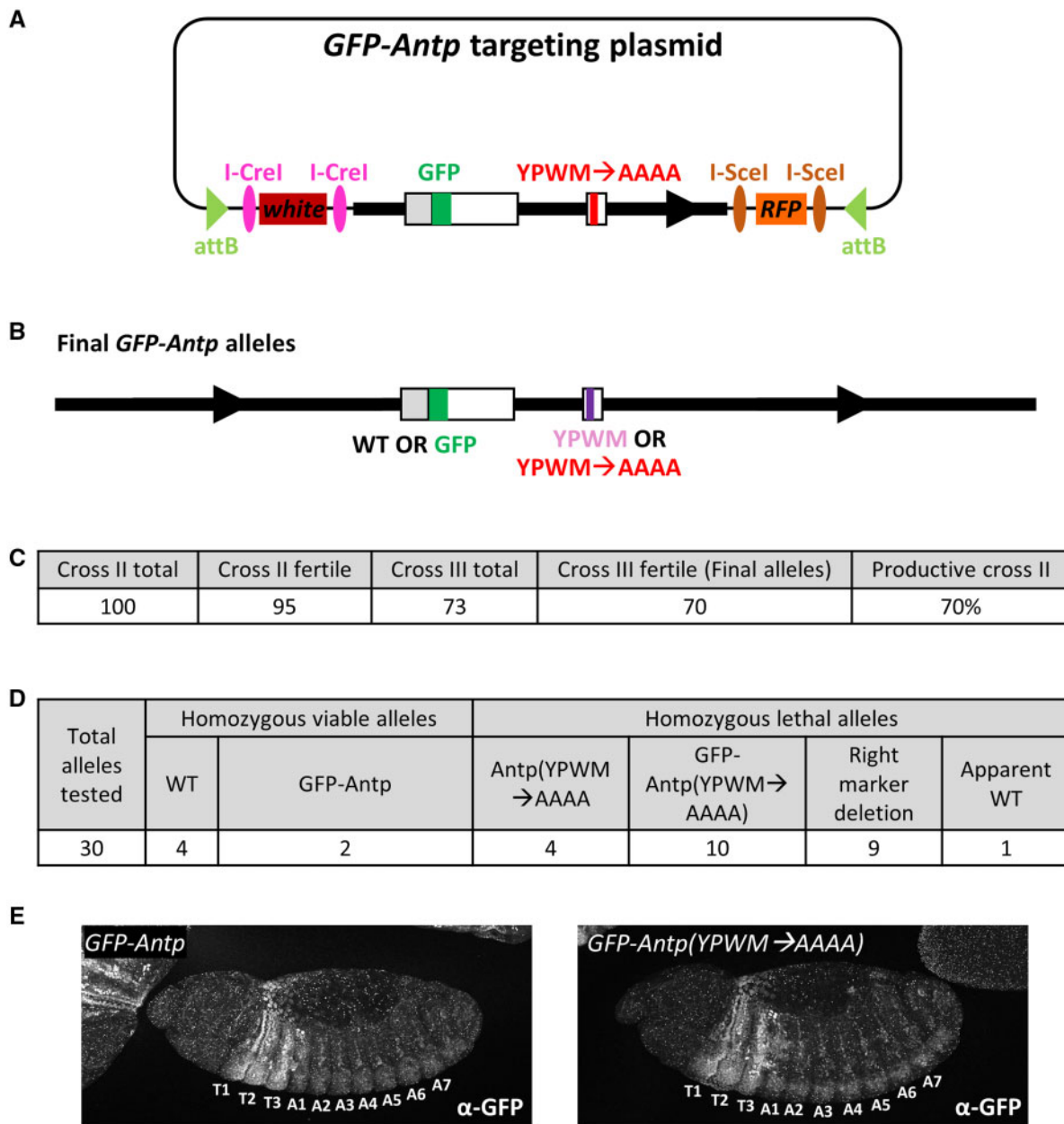


**Figure 6** Generating a precise insertion at the *Antp* locus. (A) The *GFP-Antp* targeting plasmid. The *GFP* insertion and the YPWM→AAAA mutation are indicated. (B) Desired final *GFP-Antp* alleles. The schematics in A and B are not drawn to scale. (C) Results of simultaneous resolution of the selected *GFP-Antp* RMCE allele. (D) Genotyping results of 30 selected *GFP-Antp* targeting final alleles. (E) Anti-GFP staining of *GFP-Antp* and *GFP-Antp*(YPWM→AAAA) embryos. The embryos may be homozygous, or heterozygous with *TM6B*. Segments T1 to A7 are shown.

chromosome. Indeed, genetic crosses indicated the presence of a second *MiMIC* insertion on chromosome IV (data not shown).

Nevertheless, we obtained three independent RMCE events at the desired *MI11240* insertion. Two alleles, A and B, inserted in the opposite orientation, while allele C was *white+*, *yellow-*, but *RFP-*. The lack of *RFP* in allele C might be due to spontaneous resolution of the right side induced by the dsDNA breaks generated by the  $\phi$ C31 integrase during RMCE. Indeed, Southern blot results supported this idea (data not shown), and this allele was essentially equivalent to a right-side resolved allele.

All three RMCE alleles were subjected to simultaneous resolution (Supplementary Figure S6). Multiple independent stocks were obtained from each RMCE line, but compared with the other targeting experiments described above, a notable reduction in

efficiency was observed (Figure 7D), likely because the distance between the dsDNA break and the left homologous arm was >7 kb (Figure 7, A and B; Gao et al. 2008).

All final alleles were homozygous viable and fertile, and the homozygotes were verified in several steps (Figure 7E). First, the presence of the desired deletion was determined by PCR using primers flanking the deletion. Next, those alleles that generated the correctly sized PCR product were subjected to additional PCRs using two pairs of primers against different regions of the deleted fragment. Several alleles derived from RMCE lines A and B produced positive products for all of these PCRs, suggesting that complex rearrangements occurred during resolution. Three independent final alleles, all from RMCE line C, passed all PCR tests, and all three were further verified by Southern blot



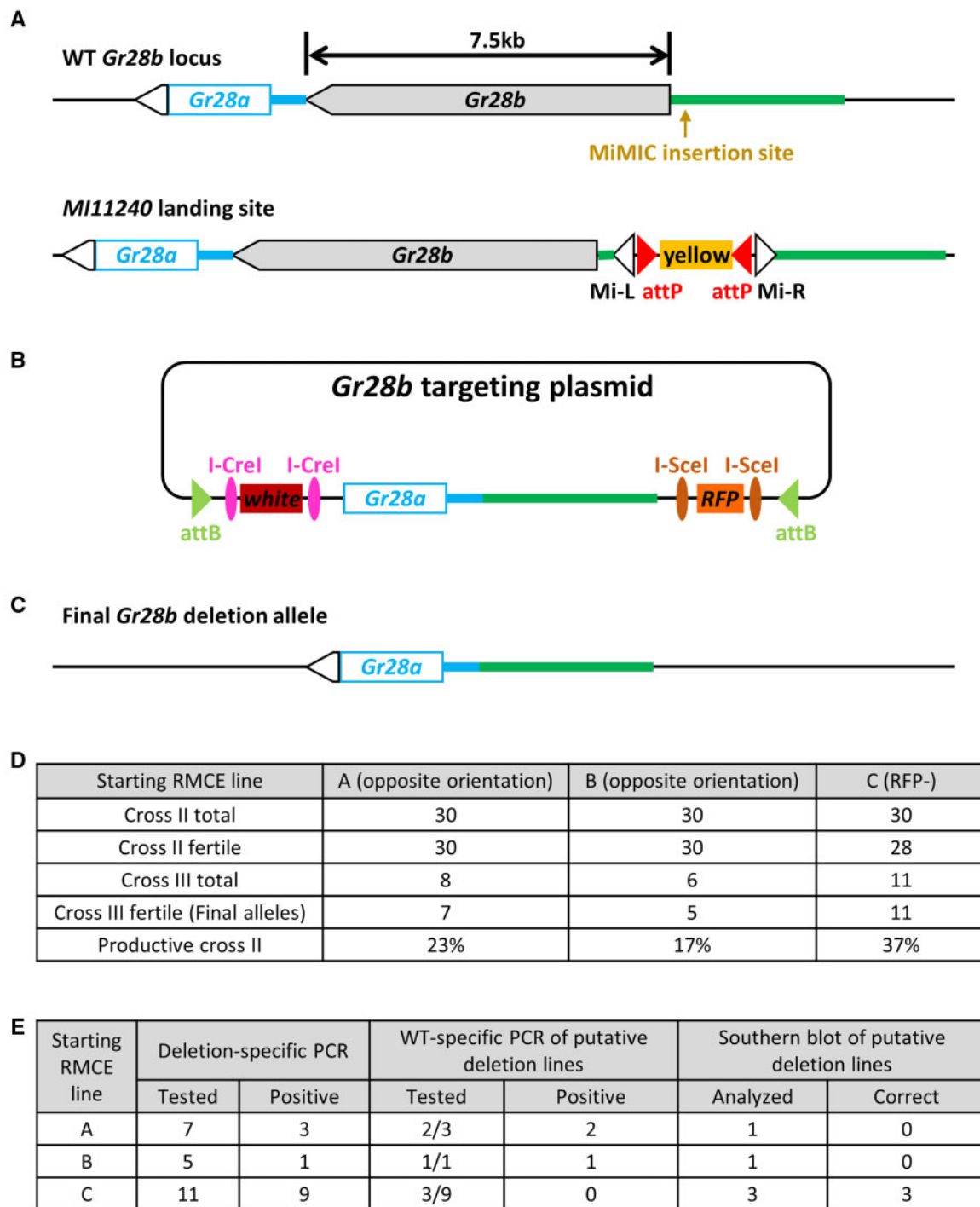


**Figure 7** The precise deletion of the 7.5 kb *Gr28b* gene. (A) Schematics showing the wild type *Gr28b* locus and the chromosome bearing the selected MiMIC landing site. (B) The targeting plasmid containing an integrated fragment with the desired deletion. (C) Schematic of the desired *Gr28b* deletion allele. The schematics in (A–C) are not drawn to scale. (D) Simultaneous resolution results of all three RMCE alleles obtained from injection. Two RMCE alleles have the opposite orientation while the third likely underwent spontaneous right-side resolution during RMCE (see text for more details). (E) The genotyping results of selected *Gr28b* deletion final alleles.

(Supplementary Figure S10) and sequencing. Thus, despite a sub-optimal initial RMCE step, this technique was able to generate a large 7.5 kb custom deletion.

## Discussion

In the past several decades, research using model organisms has greatly advanced our understanding of biology. Currently,

knock-out lines exist for most genes in well studied model organisms, and for future research, precise mutations, such as those affecting only a specific part of a protein, are often necessary to further elucidate the molecular mechanisms underlying various biological processes. Because any scar sequences left in the genome after custom mutagenesis might have unwanted consequences and could confound subsequent analyses, scarless engineering of the genome is often preferred. Here, we describe a

novel technique that is able to easily and efficiently generate scarless custom mutant alleles in the model organism *D. melanogaster*.

### Advantages of this technique

The advances of CRISPR-based techniques have made the engineering of the *Drosophila* genome much easier, but many custom mutant alleles generated with CRISPR still contain sequence scars. Although generating scarless custom mutations in *Drosophila* is feasible, significant effort is required. And regardless of which CRISPR strategy is used, a major uncertainty is that the selected gRNA(s) might be inefficient, or even nonfunctional. The technique presented here avoids this uncertainty and uses RMCE, a procedure proven to be robust and efficient, to target genomic sequences near the selected landing site.

This technique is simple and fast. The dominant markers ensure the easy identification of desired individuals in each step, and no laborious screening is necessary. If performing the simultaneous resolution, the desired stocks could be obtained in <2 months from the starting RMCE lines.

This technique generates scarless mutant alleles very efficiently. If the desired genomic alterations are not large deletions that necessitate long distances between the dsDNA breaks and the homologous arms during resolution, at least 1/3 of the cross IIs are expected to be productive, and this rate of success is usually much higher, and can even be over 70%. Fifty independent cross IIs should assure the successful generation of the desired allele. If multiple combinations of 2 separate modifications at the locus of interest are desired, such as in our *Hox* targeting experiments, increasing the number of cross IIs to 100 should ensure that all desired genotype combinations will be obtained. In fact, this technique is especially suitable for generating multiple combinations of discrete modifications at the locus of interest. Only one injection is performed to obtain an RMCE allele that contains all individual modifications, and the final alleles of all different genotype combinations can be obtained.

This technique is also very robust. Microinjection is a necessary step of essentially any *Drosophila* genome engineering attempt, but microinjection has the potential to result in significant variability. Many factors, such as landing site location, or the presence of a second landing site such as in the case of the *Gr28b* deletion, could lead to suboptimal RMCE injection results. Even if only RMCE lines with opposite orientation, or only lines with spontaneous resolution are obtained and have to be used, the desired alleles can still be generated. The robustness also means that even difficult mutations, such as large deletions, could be generated with this technique, although the efficiencies are expected to be lower compared with simpler modifications.

### This technique can engineer the majority of the *Drosophila* genome

In this study, we did not systematically test how far away from the landing site can be reached and efficiently engineered by this technique. But from previous reports of homing nuclease-mediated resolution of local duplications, we estimate that any sequence within 5 kb from the landing site could be efficiently engineered (Rong et al. 2002; Gao et al. 2008), and sequences as far as 70 kb or even further from the landing site might be engineerable (Wesolowska and Rong 2013). During resolution, the chromatin could be resolved either to the wild type sequence, or the desired mutant sequence, and the frequency of getting the mutant allele depends on the lengths of the homologous arms, and the distance between the landing site and the locus to be

engineered. For loci far from the landing site, it would likely be helpful to increase the length of the homologous arms in the targeting plasmid, such that the arms extend well beyond the locus to be engineered.

There are 17,500 MiMIC insertions (Venken et al. 2011; Nagarkar-Jaiswal et al. 2015; Lee et al. 2018) and hundreds of CRIMIC lines (which is steadily increasing; Lee et al. 2018) that are available to the fly community. Of the 17,500 MiMIC insertions, the locations of 7441 are available online (<http://flypush.imgen.bcm.tmc.edu/pscreen/downloads.html>). 56.7 Mb of euchromatic fly genome lies <5kb from a mapped MiMIC insertion (see *Materials and Methods* for the calculation), thus the currently available mapped MiMIC insertions provide efficient access to about half of the 117 Mb euchromatic fly genome (Hoskins et al. 2015) by this method. About 887 kb of heterochromatin is also expected to be accessible. Moreover, these mapped MiMIC insertions represent only a subset of all available insertions containing inverted attP cassettes, and insertions with single attP sites, or even FRT sites, are also potential landing sites (see below). Finally, the 5 kb limit for genome modification is also a conservative estimate. Taken together, we estimate that with available landing sites, this method could be used to precisely engineer the majority of the fly genome in a scarless manner. In case there is no suitable landing site near the locus of interest, such as our engineering the *Ubx* locus, a custom landing site can be generated to facilitate scarless genome editing.

### Sequential resolution vs simultaneous resolution

We have tested two different resolution strategies, sequential resolution and simultaneous resolution. Simultaneous resolution is much faster and can generate the desired alleles from the RMCE lines in <2 months. Sequential resolution, on the other hand, takes longer because the one-side resolved alleles must be verified before the second side is resolved. The sequential resolution strategy, however, offers higher efficiency. Except for difficult mutations, essentially over 90% of independent cross IIs were successful, and the failures were only due to sterile male flies. Therefore, when difficult mutations, such as large insertions or deletions, are to be generated, a sequential resolution strategy might be preferred. In fact, to generate the 7.5 kb *Gr28b* gene, all correct deletion alleles were obtained by sequential resolution, except that the first resolution occurred spontaneously during RMCE. When performing sequential resolution, the starting RMCE lines must have the correct orientation, but RMCE lines with the opposite orientation can be used for simultaneous resolution, without an apparent decrease in efficiency.

### Potential extensions of this technique

In this study, only inverted attP cassettes were used as landing sites. It has previously been reported that for homing nuclease-mediated resolution of local duplications, resolution efficiency inversely correlated with the distance between homologous arms on chromatin and dsDNA breaks (Gao et al. 2008). Landing sites with inverted attP cassettes are expected to give the highest resolution efficiency, because when RMCE lines from these landing sites are subjected to homing nuclease-mediated resolution, only short nonhomologous sequences exist between the dsDNA breaks and the homologous arms. However, this does not mean that only inverted attP cassettes can be used as landing sites. Transposon insertions containing a single attP site are also valid landing sites. When using a single attP site as the landing site, the entire targeting plasmid will be integrated into the genome via  $\phi$ C31 integrase-mediated site-specific recombination.

The targeting plasmid backbone, as well as extra sequences present in the original attP-containing transposon, will increase the distances between homologous arms on chromatin and the dsDNA breaks. This will likely lead to a decreased resolution efficiency, and aberrant rearrangements might be more frequent (Gao et al. 2008). Nevertheless, given the high efficiency of this technique, we expect that the desired alleles can still be generated.

In addition, flippase-mediated recombination between FRT sites has been used to integrate plasmids into the *Drosophila* genome in a site-specific manner (Horn and Handler 2005). In principle, FRT sites could also be used as an initial landing site for this method. However, due to the bidirectional nature of recombination between FRT sites, the plasmid integration efficiency would be expected to be lower than the unidirectional attB-attP integration mediated by phiC31 integrase. Once successful integration events are obtained, the resolution step should work equally well compared with attB-attP integration events. Targeting vectors for single attP and FRT landing sites have been generated (Supplementary Figure S2).

The general principle we demonstrate in this study is that any genomic locus can be engineered in a scarless manner if a DNA fragment can be integrated nearby. Due to the highly conserved homologous recombination pathways, we expect this principle to be applicable to other organisms.

## Acknowledgments

We would like to thank Yikang Rong for the *hs-I-SceI* fly line, Al Handler for the pXLBacII-pUbDsRed-T3 plasmid, and Susan Parkhurst for the p[sChFP] plasmid. We thank Timothy J. Dahlem for his help with the design and production of the TALEN encoding plasmids. We also want to thank all past and present members in the Mann lab for insightful discussions.

## Funding

This study was supported by NIH Grant 5R21NS105507-02 to W.B.G and NIH grant R35GM118336 to R.S.M. The content of this publication is solely the responsibility of the authors and does not necessarily represent the official views of the National Institutes of Health.

## Conflicts of interest

None declared.

## Literature cited

- Abreu-Blanco MT, Verboon JM, Liu R, Watts JJ, Parkhurst SM. 2012. *Drosophila* embryos close epithelial wounds using a combination of cellular protrusions and an actomyosin purse string. *J Cell Sci*. 125:5984–5997.
- Barolo S, Carver LA, Posakony JW. 2000. GFP and  $\beta$ -galactosidase transformation vectors for promoter/enhancer analysis in *Drosophila*. *BioTechniques*. 29:726–732.
- Bateman JR, Lee AM, Wu C. T. 2006. Site-specific transformation of *Drosophila* via phiC31 integrase-mediated cassette exchange. *Genetics*. 173:769–777.
- Bellaiche Y, Mogila V, Perrimon N. 1999. I-SceI endonuclease, a new tool for studying DNA double-strand break repair mechanisms in *Drosophila*. *Genetics*. 152:1037–1044.
- Beumer KJ, Trautman JK, Mukherjee K, Carroll D. 2013. Donor DNA utilization during gene targeting with zinc-finger nucleases. *G3*. 3:657.
- Bischof J, Maeda RK, Hediger M, Karch F, Basler K. 2007. An optimized transgenesis system for *Drosophila* using germ-line-specific  $\phi$ C31 integrases. *Proc Natl Acad Sci U S A*. 104:3312–3317.
- Brand AH, Perrimon N. 1993. Targeted gene expression as a means of altering cell fates and generating dominant phenotypes. *Development*. 118:401–415.
- Carroll SB, Laymon RA, McCutcheon MA, Riley PD, Scott MP. 1986. The localization and regulation of Antennapedia protein expression in *Drosophila* embryos. *Cell*. 47:113–122.
- Delker RK, Ranade V, Loker R, Voutev R, Mann RS. 2019. Low affinity binding sites in an activating CRM mediate negative autoregulation of the *Drosophila* Hox gene Ultrabithorax. *PLoS Genet*. 15: e1008444.
- Dura JM, Ingham P. 1988. Tissue- and stage-specific control of homeotic and segmentation gene expression in *Drosophila* embryos by the polyhomeotic gene. *Development*. 103:733–741.
- Gao G, McMahon C, Chen J, Rong YS. 2008. A powerful method combining homologous recombination and site-specific recombination for targeted mutagenesis in *Drosophila*. *Proc Natl Acad Sci U S A*. 105:13999–14004.
- Gratz SJ, Ukken FP, Rubinstein CD, Thiede G, Donohue LK, et al. 2014. Highly specific and efficient CRISPR/Cas9-catalyzed homology-directed repair in *Drosophila*. *Genetics*. 196:961–971.
- Handler AM, Harrell RA. 1999. Germline transformation of *Drosophila melanogaster* with the piggyBac transposon vector. *Insect Mol Biol*. 8:449–457.
- Handler AM, Harrell RA. 2001. Polyubiquitin-regulated DsRed marker for transgenic insects. *Biotechniques*. 31:824–828.
- Horn C, Handler AM. 2005. Site-specific genomic targeting in *Drosophila*. *Proc Natl Acad Sci U S A*. 102:12483–12488.
- Horn C, Jaunich B, Wimmer EA. 2000. Highly sensitive, fluorescent transformation marker for *Drosophila* transgenesis. *Dev Genes Evol*. 210:623–629.
- Hoskins RA, Carlson JW, Wan KH, Park S, Mendez I, et al. 2015. The Release 6 reference sequence of the *Drosophila melanogaster* genome. *Genome Res*. 25:445–458.
- Kanca O, Zirin J, Garcia-Marques J, Knight SM, Yang-Zhou D, et al. 2019. An efficient CRISPR-based strategy to insert small and large fragments of DNA using short homology arms. *eLife*. 8:e51539.
- Lee P-T, Zirin J, Kanca O, Lin W-W, Schulze KL, et al. 2018. A gene-specific T2A-GAL4 library for *Drosophila*. *eLife*. 7:e35574.
- Lelli KM, Noro B, Mann RS. 2011. Variable motif utilization in homeotic selector (Hox)-cofactor complex formation controls specificity. *Proc Natl Acad Sci U S A*. 108:21122–21127.
- Mann RS, Lelli KM, Joshi R. 2009. Hox specificity unique roles for cofactors and collaborators. *Curr Top Dev Biol*. 88:63–101.
- Merabet S, Mann RS. 2016. To be specific or not: the critical relationship between Hox And TALE proteins. *Trends Genet*. 32: 334–347.
- Merabet S, Saadaoui M, Sambrani N, Hudry B, Pradel J, et al. 2007. A unique extradenticle recruitment mode in the *Drosophila* Hox protein Ultrabithorax. *Proc Natl Acad Sci U S A*. 104:16946–16951.
- Nagarkar-Jaiswal S, Lee P-T, Campbell ME, Chen K, Anguiano-Zarate S, et al. 2015. A library of MiMICs allows tagging of genes and reversible, spatial and temporal knockdown of proteins in *Drosophila*. *eLife*. 4:e05338.
- Ni L, Bronk P, Chang EC, Lowell AM, Flam JO, et al. 2013. A gustatory receptor paralogue controls rapid warmth avoidance in *Drosophila*. *Nature*. 500:580–584.

- Port F, Muschalik N, Bullock SL. 2015. Systematic evaluation of *Drosophila* CRISPR tools reveals safe and robust alternatives to autonomous gene drives in basic research. *G3*. 5:1493.
- Rong YS, Titen SW, Xie HB, Golic MM, Bastiani M, et al. 2002. Targeted mutagenesis by homologous recombination in *D. melanogaster*. *Genes Dev*. 16:1568–1581.
- Sang J, Rimal S, Lee Y. 2019. Gustatory receptor 28b is necessary for avoiding saponin in *Drosophila melanogaster*. *EMBO Rep*. 20: e47328.
- Thummel CS, Boulet AM, Lipshitz HD. 1988. Vectors for *Drosophila* P-element-mediated transformation and tissue culture transfection. *Gene*. 74:445–456.
- Venken KJT, Schulze KL, Haelterman NA, Pan H, He Y, et al. 2011. MiMIC: a highly versatile transposon insertion resource for engineering *Drosophila melanogaster* genes. *Nat Methods*. 8: 737–743.
- Vilain S, Vanhauwaert R, Maes I, Schoovaerts N, Zhou L, et al. 2014. Fast and efficient *Drosophila melanogaster* gene knock-ins using MiMIC transposons. *G3*. 4:2381.
- Wesolowska N, Rong YS. 2013. Long-range targeted manipulation of the *Drosophila* genome by site-specific integration and recombinational resolution. *Genetics*. 193:411–419.
- Zolotarev N, Georgiev P, Maksimenko O. 2019. Removal of extra sequences with I-SceI in combination with CRISPR/Cas9 technique for precise gene editing in *Drosophila*. *Biotechniques*. 66: 198–201.

Communicating editor: Y.S. Rong